Phase-field model for Marangoni convection in liquid-gas systems with a deformable interface

Rodica Borcia* and Michael Bestehorn
Lehrstuhl für Theoretische Physik II, Brandenburgische Technische Universität Cottbus, Erich-Weinert-Straße 1, 03046 Cottbus, Germany
(Received 9 July 2002; published 26 June 2003)

We developed a phase-field model for Marangoni convection in a liquid-gas system with a deformable interface, heated from below. In order to describe both Marangoni instabilities (with short and long wavelengths), an additional force component must be considered in the Navier-Stokes equation. This term describes the coupling of the temperature to the velocity field via the phase-field function. It results by minimizing the free-energy functional of the system. For a bidimensional problem in linear approximation we performed a numerical code that successfully computes both Marangoni instabilities. In the limit of sharp and rigid interfaces, our results are compared with the literature.

DOI: 10.1103/PhysRevE.67.066307 PACS number(s): 47.20.Dr, 68.03.−g, 47.54.+r, 05.70.Np

I. INTRODUCTION

Convective cells, discovered by Bénard in his famous experiments on thin oil layers heated from below at the end of 19th century [1] (and theoretically explained by ''Marangoni forces'' caused by surface tension gradients), continue to be a challenging topic of immense interest since the past few years [2–9].

For a liquid-gas system with a nondeformable interface, maintained in themperature gradient, the termocapillarity effects induce an instability at a wave number $k \approx 2$ (scaled by liquid depth d). This instability is named the short-wavelength instability, because the spatial scale of cellular convective motions corresponds to the scale of liquid layer depth. A deformational liquid-gas interface allows for a second type of instability induced by surface deformations and called the long wave instability. This second instability develops around $k=0$, the spatial scale of convection generated by the deformational mode is much larger than the depth of the liquid layer.

In the usual description, concerning Marangoni instabilities, the Navier-Stokes (NS) equation and the heat equation are written twice: once for the liquid and once for the gas bulk. In addition, boundary conditions are imposed at the interface.

In this paper, we have analyzed the problem of Marangoni convection (MC) in a liquid-gas system with a deformable interface, heated from below, but using the phase-field model, a model new for this kind of problem. Using this phenomenological continuum model, proposed for the first time by Langer [10], we have written the NS equation and the heat equation only once, avoiding the interface conditions.

In the phase-field method one introduces an order parameter, called the phase-field function φ, to characterize thermodynamically the phases. The phase field takes distinct values in each bulk phase and undergoes a rapid but smooth variation in the interface region. The phase field φ is governed by a partial differential equation that guarantees, in the limit of a suitable thin interfacial width, that the realistic interface conditions are satisfied. With the help of the phase-field function the system is treated continuously, leading thus to a problem free of interface conditions. It can be successful in many instances with complex structures such as those present during dendritic growths [11,12] or dynamic fractures [13].

Recently, a very similar method—the so-called ghost fluid method—was developed by Osher and collaborators for describing interfaces in multimaterial flows [14,15]. In place of the phase-field function, they use a level set function to keep track of the interface. The zero level marks the location of the interface, the positive values correspond to one fluid, and the negative ones to the other. They capture the appropiate interface conditions by defining a ghost fluid (for each of the two fluids), which has at each point the same pressure and velocity of the real fluid, but the entropy of the other one. Since the ghost fluids have the same entropy as the real fluid that is not replaced, a one-phase problem is solved exactly in the same manner as in the phase-field formalism. But unlike the ghost fluid method or the classical method, in our phase-field model the interface is diffuse and, therefore, it allows a diffusive transport between the phases in the interfacial region.

We emphasize that in the present paper we are not studying a liquid in equilibrium with its own gas phase. For this case, the phase field would be the density and its spatiotemporal evolution would be described by the continuity equation. Our description introduces the phase field phenomenologically and can be used also for the case of two incompressible fluids, partially miscible. The system analyzed in this paper contains two different phases (see Fig. 1) and, how we will see in Sec. V, in the limit of sharp interfaces, our results converge to those coming from the standard formulation for flat interfaces [5].

The paper is organized as follows. In Sec. II, we describe in detail the method, we deduce the phase-field equation from the free-energy functional, and we demonstrate the necessity to introduce a new force component in the NS equation for describing Marangoni convection with a short wavelength. In the limit of sharp interfaces, the classical interface conditions for a rigid interface are derived in Sec. III. Section IV presents the basic equations used in our simulations and introduces the adimensional parameters. The numerical re-

*Electronic address: borcia@physik.tu-cottbus.de

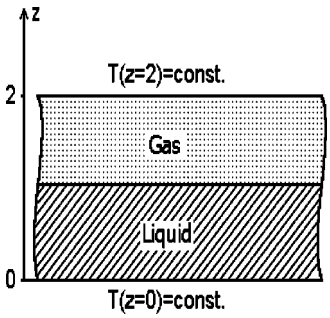

FIG. 1. Sketch of the system under consideration: a gas layer superposed over a liquid layer. The system is heated from below and the temperatures at the top and at the bottom are maintained constant.

sults concerning MC described for a bidimensional problem in linear approximation are discussed in Sec. V. Finally, our principal conclusions are summarized in Sec. VI.

II. THE SYSTEM

In our phase-field model for convective motions in a liquid-gas system, the order parameter φ is assumed to be $\varphi=-1$ at the liquid boundary ($z=0$) and $\varphi=+1$ at the gas boundary ($z=2$) (see Fig. 2). The Helmoltz free-energy functional is given by [10,16,17]

$$\mathcal{F}=\int_V\left[f(\varphi)+\frac{\mathcal{K}(T)}{2}(\vec{\nabla}\varphi)^2\right]dV, \tag{1}$$

where $f(\varphi)$ represents the free-energy density of a homogeneous fluid, describing the regions far from interphases. For $f(\varphi)$ a continuous function of φ is required with two local minima: one corresponding to $\varphi=-1$, for the bulk in the liquid state, and another one to $\varphi=+1$, for the bulk in the gas phase. We choose $f(\varphi)$ in the following form:

$$f(\varphi)=C\left(\frac{\varphi^4}{4}-\frac{\varphi^2}{2}\right)+\mu\varphi, \tag{2}$$

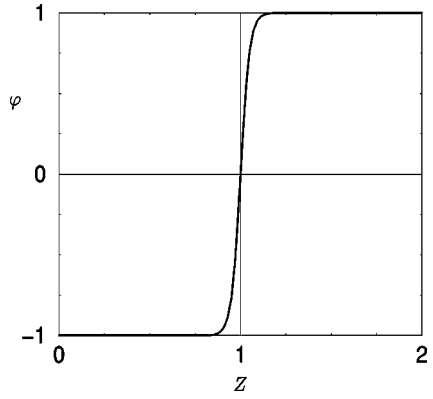

FIG. 2. Phase-field distribution versus z for the stationary state. At $z=0$ (liquid boundary), the phase-field function takes the value $\varphi=-1$ and at $z=2$ (gas boundary), the value $\varphi=+1$. The diffuse interface between liquid and gas is near $z=1$.

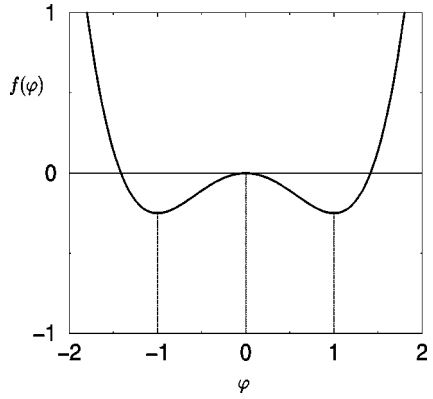

FIG. 3. Free-energy density representation versus phase-field function φ. We have chosen $f(\varphi)$ to be a symmetric ''double-well'' potential with two local minima: one at $\varphi=-1$, corresponding to the liquid phase, and the second at $\varphi=+1$, corresponding to the gas phase.

with C as a positive parameter related to interparticle potentials [18] and μ as a bias parameter related to the chemical potential. The parameter μ controls the difference between the free-energy densities corresponding to the two minima. In our model μ is considered zero, which means that both minima have the same free-energy density, as one can see from Fig. 3. The free-energy density at the interface (near $z=1$) is zero. In functional (1) appears a second term (a nonclassic term), which describes the interface phenomena (interface diffusion) [17]. This term is associated with variations of the density (and, consequently, of the phase field) and contributes to the free-energy excess of the interfacial region, which defines the surface tension coefficient [18,19]

$$\sigma=\int_{-\infty}^{+\infty}\mathcal{K}\left(\frac{\partial\varphi_0}{\partial z}\right)^2dz, \tag{3}$$

where $\varphi_0(z)$ denotes the stationary phase-field function.

In many previous works, $\mathcal{K}$ is assumed to be constant. But, for describing Marangoni convection its necessary to consider $\mathcal{K}$ to be dependent on temperature:

$$\mathcal{K}=\mathcal{K}_0-\mathcal{K}_T T \quad (\mathcal{K}_T>0), \tag{4}$$

while the temperature field is described by the usual heat equation

$$\rho c\frac{dT}{dt}=\vec{\nabla}\cdot(\kappa\vec{\nabla}T), \tag{5}$$

with ρ as the fluid density, c as the heat capacity, and κ as the thermal conductivity.

We will now derive the equation for the phase-field function φ. To this aim we differentiate the free-energy functional given by relation (1) with respect to time and impose the energy production resulting after differentiation to be negative in any subvolume ϑ of V. (In the system an irreversible phenomenon is present—the interface diffusion, resulting thus in the monotonic decrease of the free-energy density.) For the sake of simplicity, we assume for the mo-

ment a weak dependence of $\mathcal{K}$ on temperature: $\mathcal{K}\approx\mathcal{K}_0$ = const. From Eq. (1) one gets

$$\dot{\mathcal{F}}=\int_{\vartheta}\left[\frac{\partial f}{\partial\varphi}\dot{\varphi}+\mathcal{K}_0\vec{\nabla}\varphi\cdot\vec{\nabla}\dot{\varphi}\right]dV=\int_{\vartheta}\left[\frac{\partial f}{\partial\varphi}\dot{\varphi}+\vec{\nabla}\cdot(\mathcal{K}_0\dot{\varphi}\vec{\nabla}\varphi)-\mathcal{K}_0\dot{\varphi}\Delta\varphi\right]dV. \tag{6}$$

The mass conservation of the system requires

$$\dot{\varphi}=-\vec{\nabla}\cdot\vec{J}, \tag{7}$$

where $\vec{J}$ represents the diffusional flux. Substitution of Eq. (7) into Eq. (6) leads to

$$\dot{\mathcal{F}}=\int_{\mathcal{A}}\left(\mathcal{K}_0\dot{\varphi}\vec{\nabla}\varphi-\frac{\partial f}{\partial\varphi}\vec{J}+\mathcal{K}_0\Delta\varphi\vec{J}\right)\cdot\vec{n}dA+\int_{\vartheta}\vec{J}\cdot\vec{\nabla}\left(\frac{\partial f}{\partial\varphi}-\mathcal{K}_0\Delta\varphi\right)dV. \tag{8}$$

The energy production can be calculated by subtracting from $\dot{\mathcal{F}}$, from Eq. (8), the first term that describes the energy flux through the boundary of subvolume ϑ [16]:

$$\sigma_{\epsilon}=\int_{\vartheta}\vec{J}\cdot\vec{\nabla}\left(\frac{\partial f}{\partial\varphi}-\mathcal{K}_0\Delta\varphi\right)dV.$$

Choosing

$$\vec{J}=-M_o\vec{\nabla}\left(\frac{\partial f}{\partial\varphi}-\mathcal{K}_0\Delta\varphi\right), \tag{9}$$

with M_o as a positive constant, one obtains for the energy production,

$$\sigma_{\epsilon}=-\int_{\vartheta}\frac{|\vec{J}|^2}{M_o}dV\leqslant 0. \tag{10}$$

This result emphasizes the decrease in time of free-energy density due to interface diffusion. Substituting now relation (9) into Eq. (7), one gets the partial differential equation for the phase-field function φ:

$$\dot{\varphi}=-M_o\Delta\left(\mathcal{K}_0\Delta\varphi-\frac{\partial f}{\partial\varphi}\right), \tag{11}$$

known in the literature as the Cahn-Hilliard (CH) equation [20].

In order to introduce the contribution of the phase field in the Navier-Stokes equation, we apply the Lagrangian formalism. Thus, in order to minimize the free-energy functional for the equilibrium state, the Lagrangian energy density

$$\mathcal{L}(\mathcal{K}(T),\varphi,\vec{\nabla}\varphi)=f(\varphi)+\frac{\mathcal{K}(T)}{2}(\vec{\nabla}\varphi)^2 \tag{12}$$

must satisfy the Euler-Lagrange equation

$$\frac{\partial\mathcal{L}}{\partial\varphi}-\frac{\partial}{\partial x_i}\left(\frac{\partial\mathcal{L}}{\partial(\partial_i\varphi)}\right)=0. \tag{13}$$

Substitution of Eq. (12) into Eq. (13) gives us the following relation (Noether's theorem):

$$\frac{\partial}{\partial x_i}\left[\frac{\partial\mathcal{L}}{\partial(\partial_i\varphi)}\frac{\partial\varphi}{\partial x_j}-\mathcal{L}\delta_{ij}\right]+\frac{\partial\mathcal{L}}{\partial\mathcal{K}}\frac{\partial\mathcal{K}}{\partial x_i}\delta_{ij}=0, \tag{14}$$

with $j=1,2,3$.

Assuming $\mathcal{K}=$ const, from the above equation, the stress tensor appears [17,21] to be

$$\vec{\vec{\Xi}}=\mathcal{K}\vec{\nabla}\varphi\otimes\vec{\nabla}\varphi-\mathcal{L}\mathcal{I}, \tag{15}$$

in components

$$\Xi_{ij}=\mathcal{K}\frac{\partial\varphi}{\partial x_i}\frac{\partial\varphi}{\partial x_j}-\mathcal{L}\delta_{ij},$$

which satisfies the conservation law

$$\vec{\nabla}\cdot\vec{\vec{\Xi}}=0. \tag{16}$$

Because the Navier-Stokes equation expresses the momentum conservation law, the contribution of capillary forces in this equation is given by the conservative term $-\vec{\nabla}\cdot\vec{\vec{\Xi}}$, leading thus to [22]

$$\rho\frac{d\vec{v}}{dt}=\vec{\nabla}(-p+\mathcal{L})-\vec{\nabla}\cdot(\mathcal{K}\vec{\nabla}\varphi\otimes\vec{\nabla}\varphi)+\vec{\nabla}\cdot(\eta\vec{\nabla}\vec{v})+\rho g\hat{z} \tag{17}$$

(both fluids are assumed incompressible).

But, when $\mathcal{K}\neq$ const, the conservative law (16) is not satisfied, we must consider also the last term of relation (14). Using Eqs. (12) and (4) one gets, respectively,

$$\frac{\partial\mathcal{L}}{\partial\mathcal{K}}=\frac{1}{2}(\vec{\nabla}\varphi)^2,$$

$$\frac{\partial\mathcal{K}}{\partial x_i}=\frac{\partial\mathcal{K}}{\partial T}\frac{\partial T}{\partial x_i}=-\mathcal{K}_T\frac{\partial T}{\partial x_i}.$$

Therefore, when $\mathcal{K}\neq$ const, a new force component has to be included in the NS equation, which represents, in fact the driver of MC with a short wavelength (caused by surface tension gradient), indicated by the last term in the following equation:

$$\rho\frac{d\vec{v}}{dt}=\vec{\nabla}(-p+\mathcal{L})-\vec{\nabla}\cdot(\mathcal{K}\vec{\nabla}\varphi\otimes\vec{\nabla}\varphi)+\vec{\nabla}\cdot(\eta\vec{\nabla}\vec{v})+\rho g\hat{z}+\frac{1}{2}\mathcal{K}_T\vec{\nabla}T(\vec{\nabla}\varphi)^2. \tag{18}$$

Finally, we note that in the case of a single-component fluid, a more rigorous derivation would be to consider the density ρ as the phase variable [φ has to be replaced by ρ in Eq. (18)]. The fluid must be treated as being compressible and

instead of the Cahn-Hilliard equation (11) introduced phenomenologically above, the continuity equation determines the temporal evolution of the phase field:

$$\frac{d\rho}{dt} = -\rho\vec{\nabla}\cdot\vec{v} = -\vec{\nabla}\cdot(\vec{\nabla}\Phi), \tag{19}$$

where the potential function Φ describes the compressible part of the velocity field

$$\vec{v} = \vec{\nabla}\times(\psi\vec{e}_y) + \vec{\nabla}\Phi$$

and the stream function ψ as the incompressible one, as one can see in Sec. V. To obtain the Cahn-Hilliard equation, one may assume that the compressible part of the velocity is proportional to the gradient of the chemical potential at the interface which, in turn, is given by the functional derivative of the free energy (1) (for completeness, $\mathcal{F}$ must be considered as function of ρ):

$$\vec{\nabla}\Phi = -M_o\vec{\nabla}\frac{\delta\mathcal{F}}{\delta\rho}, \tag{20}$$

with M_o as the mobility. Inserting Eq. (20) in Eq. (19) finally yields the Cahn-Hilliard equation (11). It is clear that this derivation is not systematic and the application of the Cahn-Hilliard equation can be considered as a model. The advantage of our model is that it can be used also in two immiscible fluids having the same density, separated by a narrow but diffuse interface. Then, ρ is a constant (incompressible) even across the interface, but φ can still be used as the phase variable.

III. SHARP-INTERFACE LIMIT

In this section, in the limit of sharp and rigid interface, we derive the ''classical interface conditions'' for a two-fluid system with surface tension gradients at the interface. In this way, one proves the necessity to introduce in our phase-field model the new term $\frac{1}{2}\mathcal{K}_T\vec{\nabla}T(\vec{\nabla}\varphi)^2$ in the NS equation (18), responsible for describing the Marangoni instability induced by thermocapillarities.

We have analyzed in this paper a bidimensional problem, considering the fluid parameters depending on (x,z) coordinates.

One can integrate Eq. (18) through a flat and rigid interface ($\partial\varphi/\partial x = 0$) between the limits $1-\varepsilon$ and $1+\varepsilon$ (see Fig. 4). For a weak dependence of $\mathcal{K}$ on temperature, in the limit $\varepsilon\to 0$, one obtains for the z component,

$$\int_{1-\varepsilon}^{1+\varepsilon}\eta\triangle v_z dz = \mathcal{K}\left(\frac{\partial\varphi}{\partial z}\right)^2\Bigg|_{1-\varepsilon}^{1+\varepsilon}.$$

For sharp interfaces ($\partial\varphi/\partial z|_{z=1-\varepsilon} = \partial\varphi/\partial z|_{z=1+\varepsilon} = 0$), the right-hand side term of the above equation vanishes, leading thus to the identity

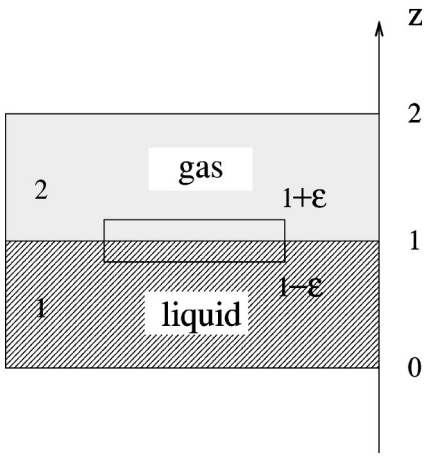

FIG. 4. Sketch of the system under discussion: a contour through the liquid-gas interface is considered. In the limit of sharp interfaces, integrating NS equation (18) along this contour, we have derived the classical interface conditions when $\varepsilon\to 0$.

$$\int_{1-\varepsilon}^{1+\varepsilon}\eta\Delta v_z dz = \eta_l\int_{1-\varepsilon}^{1}\Delta v_z dz + \eta_g\int_{1}^{1+\varepsilon}\Delta v_z dz = 0. \tag{21}$$

Identity (21) is satisfied for any positive values for liquid and gas viscosities. Therefore, we have

$$\Delta v_z = 0, \quad 1-\varepsilon \leqslant z \leqslant 1,$$
$$\Delta v_z = 0, \quad 1 \leqslant z \leqslant 1+\varepsilon \tag{22}$$

for any positive ε ($\varepsilon\to 0$).

From Eq. (22), one gets finally

$$v_z = 0 \tag{23}$$

in the vicinity of $z=1$, a relation which expresses the nondeformability condition [23]. Integrating now the x component of the NS equation, with the same assumptions as in the preceding case, using the nondeformability condition (23), too, one arrives at

$$\int_1^2\frac{\partial}{\partial z}\left(\eta\frac{\partial v_x}{\partial z}\right)dz = -\frac{\mathcal{K}_T}{2}\frac{\partial T}{\partial x}\int_1^2\left(\frac{\partial\varphi_0}{\partial z}\right)^2 dz \tag{24}$$

(the notations ''1'' and ''2'' correspond to Fig. 4). In the right-hand side of relation (24), we will introduce a temperature-dependent surface tension coefficient with the help of relation (3), which can be also written in the following form [18]:

$$\sigma \approx \tfrac{2}{3}\sqrt{(\mathcal{K}_0 - \mathcal{K}_T T)C}. \tag{25}$$

From Eq. (25) results immediately

$$\left|\frac{\partial\sigma}{\partial T}\right| = \frac{\sigma\mathcal{K}_T}{2\mathcal{K}}. \tag{26}$$

Substituting now relations (3), (25), and (26) into Eq. (24), we obtain the interface condition for tangential stresses [23]

$$\sigma'_{xz}(2)-\sigma'_{xz}(1)=\frac{\partial\sigma}{\partial x}, \tag{27}$$

where $\sigma'_{xz}=\eta[(\partial v_x/\partial z)+(\partial v_z/\partial x)]$ is the viscous tensor for incompressible fluids.

We must stress here on the importance of the new force component $\frac{1}{2}\mathcal{K}_T\vec{\nabla}T(\vec{\nabla}\varphi)^2$ introduced in Eq. (18). This term is responsible for the appearance of a surface tension gradient $\partial\sigma/\partial x$ in the interface condition (27) and plays essential role in the mechanism of forming MC with a short wavelength.

In addition to the nondeformability condition (23) and the interface condition for tangential stresses (27), we can easily derive the heat-flux continuity at the interface [23], applying the same procedure for NS equation (18) for the heat equation (5). One thus gets

$$\left(\kappa\frac{\partial T}{\partial z}\right)(1)=\left(\kappa\frac{\partial T}{\partial z}\right)(2), \tag{28}$$

where the notations ''1'' and ''2'' correspond again to Fig. 4.

IV. BASIC EQUATIONS

Summarizing, the fundamental set of equations describing the convective phenomena in a two-fluid system reads

$$\rho\frac{d\vec{v}}{dt}=\vec{\nabla}(-p+\mathcal{L})-\vec{\nabla}\cdot(\mathcal{K}\vec{\nabla}\varphi\otimes\vec{\nabla}\varphi)+\frac{1}{2}\mathcal{K}_T\vec{\nabla}T(\vec{\nabla}\varphi)^2$$
$$+\vec{\nabla}\cdot(\eta\vec{\nabla}\vec{v})+\rho g\hat{z},$$
$$\frac{d\varphi}{dt}=-M_o\Delta\left(\mathcal{K}\Delta\varphi-\frac{\partial f}{\partial\varphi}\right), \tag{29}$$
$$\rho c\frac{dT}{dt}=\vec{\nabla}\cdot(\kappa\vec{\nabla}T),$$
$$\vec{\nabla}\cdot\vec{v}=0,$$

where the density $\rho(x,z,t)$, the viscosity $\eta(x,z,t)$, the heat capacity $c(x,z,t)$, and the thermal conductivity $\kappa(x,z,t)$ are assumed to vary from the liquid to the gas bulk through linear functions of the phase field $\varphi(x,z,t)$:

$$\rho=\frac{\rho_0+\rho_1}{2}-\frac{\rho_0-\rho_1}{2}\varphi,\quad \eta=\frac{\eta_0+\eta_1}{2}-\frac{\eta_0-\eta_1}{2}\varphi,$$
$$c=\frac{c_0+c_1}{2}-\frac{c_0-c_1}{2}\varphi,\quad \kappa=\frac{\kappa_0+\kappa_1}{2}-\frac{\kappa_0-\kappa_1}{2}\varphi.$$

In the above relations, index ''0'' describes the fluid parameters at $z=0$ (liquid boundary), while index ''1'' describes the gas parameters at $z=2$ (gas boundary).

In the NS equation, we apply the curl operator in order to eliminate the gradient term $\vec{\nabla}(-p+\mathcal{L})$ and, after the following adimensionalizations:

$$\vec{r}=d\vec{r'},\quad t=\frac{d^2}{\chi_0}t',\quad \vec{v}=\frac{\chi_0}{d}\vec{v'},\quad T'=\frac{T-T_1}{T_0-T_1},$$
$$\rho=\rho_0\rho',\quad \eta=\eta_0\eta',\quad c=c_0c',\quad \kappa=\kappa_0\kappa'$$

(χ_0 is the thermal diffusivity at liquid boundary), the system of Eqs. (29) becomes (the accents are dropped)

$$\vec{\nabla}\times\left(\rho\frac{d\vec{v}}{dt}\right)=-\mathrm{Pr}\,L\vec{\nabla}\times\{\vec{\nabla}\cdot[(\mathrm{Ca}-MT)\vec{\nabla}\varphi\otimes\vec{\nabla}\varphi]$$
$$-\tfrac{1}{2}M\vec{\nabla}T(\vec{\nabla}\varphi)^2\}+\mathrm{Pr}\,\vec{\nabla}\times[\vec{\nabla}\cdot(\eta\vec{\nabla}\vec{v})]$$
$$+G\,\mathrm{Pr}\vec{\nabla}\times(\rho\hat{z}), \tag{30}$$
$$\frac{d\varphi}{dt}=-M'_o\Delta\left[L^2\left(1-\frac{MT}{\mathrm{Ca}}\right)\Delta\varphi-\varphi^3+\varphi\right],$$
$$\rho c\frac{dT}{dt}=\vec{\nabla}\cdot(\kappa\vec{\nabla}T)$$
$$\vec{\nabla}\cdot\vec{v}=0.$$

In the system of equations (30) appear the dimensionless parameters: $\mathrm{Pr}=\rho_0\chi_0/\eta_0$ is the Prandtl number of the liquid, $Ca=\sqrt{\mathcal{K}_0C}d/\eta_0\chi_0$ is the capillary number, $M=(\mathcal{K}_T\sqrt{\mathcal{K}_0C}/\mathcal{K}_0)/[(T_0-T_1)d/\eta_0\chi_0]$ is the Marangoni number, $G=\rho_0gd^3/\eta_0\chi_0$ is the Galileo number, $L=(1/d)\sqrt{\mathcal{K}_0/C}$ is the width of interface, and $M'_o=M_oC/\chi_0$ is the phenomenological mobility adimensionalized, where $\sqrt{\mathcal{K}_0C}$ has the dimension of surface tension and $\mathcal{K}_T\sqrt{\mathcal{K}_0C}/\mathcal{K}_0$ describes the temperature gradient of surface tension. All the adimensional parameters indicated above were introduced, e.g., in Ref. [5], except the last ones which are specific for our model.

V. NUMERICAL RESULTS

Because both fluids are assumed to be incompressible, in the NS equation from the system of Eqs. (30) we introduce the stream function $\psi(x,z,t)$ in place of the velocity field $\vec{v}(x,z,t)$. For the bidimensional problem (x,z) considered in this paper, one can write

$$\vec{v}=\frac{\partial\psi}{\partial z}\vec{i}-\frac{\partial\psi}{\partial x}\vec{k}.$$

We have analyzed the basic equations (30) in the linear approximation, assuming for the perturbation plane waves in the horizontal direction,

$$\begin{pmatrix}\psi(x,z,t)\\ \varphi(x,z,t)\\ T(x,z,t)\end{pmatrix}=\begin{pmatrix}\psi^{(0)}(z)\\ \varphi^{(0)}(z)\\ T^{(0)}(z)\end{pmatrix}+\begin{pmatrix}\psi^{(1)}(z)\\ \varphi^{(1)}(z)\\ T^{(1)}(z)\end{pmatrix}$$
$$\times\exp(ikx)\exp(\lambda t), \tag{31}$$

with wave number k (assumed to be real value) and the (complex) growth rate λ. After linearization one obtains a system of equations depending only on variable z, with derivatives till the fourth order. For this linearized system we have used a finite difference method [24] with a variable step, taking into account the following boundary conditions:

$$\psi^{(1)}|_{z=0} = \psi^{(1)}|_{z=2} = 0, \quad \left.\frac{\partial \psi^{(1)}}{\partial z}\right|_{z=0} = \left.\frac{\partial \psi^{(1)}}{\partial z}\right|_{z=2} = 0,$$

$$\varphi^{(1)}|_{z=0} = \varphi^{(1)}|_{z=2} = 0, \quad \left.\frac{\partial \varphi^{(1)}}{\partial z}\right|_{z=0} = \left.\frac{\partial \varphi^{(1)}}{\partial z}\right|_{z=2} = 0,$$

$$T^{(1)}|_{z=0} = T^{(1)}|_{z=2} = 0.$$

In this way, system (30) with the above boundary conditions is reduced to a linear eigenvalue problem. For the numerical results presented in this section, we have chosen the parameters for a silicon oil-air system: $\mathrm{Pr} = 10^2, \kappa_1/\kappa_0 = 0.18, \rho_1/\rho_0 = 1.7\times 10^{-3}, \eta_1/\eta_0 = 0.22\times 10^{-3}, c_1/c_0 = 0.5$ [5].

A. Nondeformable interface

At the first step we have dropped the Cahn-Hilliard equation from Eqs. (30). This means that the interface is assumed to be perfectly rigid but diffuse and, for the phase-field function which appears in the NS equation, we have considered (only for this particular situation) a variation of the form

$$\varphi^{(0)}(z) = \tanh\frac{(z-1)}{L\sqrt{2}}, \tag{32}$$

with L the parameter that describes the interface thickness. Because the interface is rigid, only one instability can appear here. This is the short-wavelength instability, driven by surface tension gradient, which develops when the Marangoni number exceeds a critical value M_{cr}.

Figure 5 shows the critical Marangoni number M_{cr} and the critical wave number k_{cr} versus $1/L$ for two different cases: case 1 corresponds to the situation when the CH equation is dropped (the interface is perfectly rigid), while case 2 corresponds to the situation when the CH equation is included. Here, large values for the capillary number Ca and the Galileo number G are assumed, the interface can be regarded as quasi-nondeformable. (For case 2 in Fig. 5 the liquid depth is of order $d \approx 10^{-2}$ m.) From the representations indicated in Fig. 5 one can see how M_{cr} and k_{cr} decrease with increasing $1/L$, arriving at a saturation in the limit of sharp interfaces (large values for $1/L$ corresponds to sharp interfaces). The critical Marangoni number saturates around $M_{cr} = 750$ and the critical wave number around $k_{cr} = 2.06$, values which are in concordance with those obtained in Ref. [5] for flat and sharp interfaces. The critical Marangoni number $M_{cr} \approx 750$ yields in terms of the usual definition [8]

$$M' = M\frac{B_i}{B_i + 1},$$

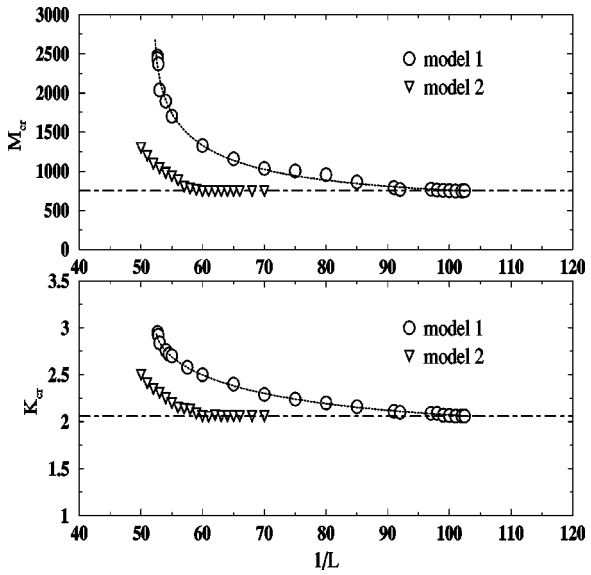

FIG. 5. Dependencies of the critical Marangoni number M_{cr} and the critical wave number k_{cr} on the interface thickness, for MC driven by a surface tension gradient. The plots correspond to two different models: model 1 assumes a perfect rigid liquid-gas interface, while in model 2 the interface is quasi-nondeformable. For model 2, one considers $\mathrm{Ca} = 2\times 10^5, G = 3\times 10^9$. Both models converge in the limit of sharp interface to classical results obtained for liquid-gas systems with flat interfaces.

(with $B_i = \kappa'/a$ as the Biot number, $\kappa' = \kappa_{gas}/\kappa_{liq}$, and $a = d_{gas}/d_{liq}$) a value around $M' \approx 110$.

For sharp interfaces (case 1), we have represented in Fig. 6 the growth rate $\mathrm{Re}\lambda$ for the Marangoni instability with short wavelength versus wave number k for the critical Marangoni number $M_{cr} = 750$. The eigenfunctions characteristic for MC with short wavelength are presented in Fig. 7 for $k = 2.06$ and for all the other parameters indicated in Fig. 6. In the left panels, the temperature and stream-function perturbations are represented versus z, while the right panels show the same perturbations in the bidimensional (x,z) representation. Figure 7(a) presents a discontinuity at the interface (near $z = 1$), which appears because the thermal conductivity in the liquid is almost one order of magnitude greater than that of the gas ($\kappa_{gas}/\kappa_{liq} = 0.18$). This discontinuity from

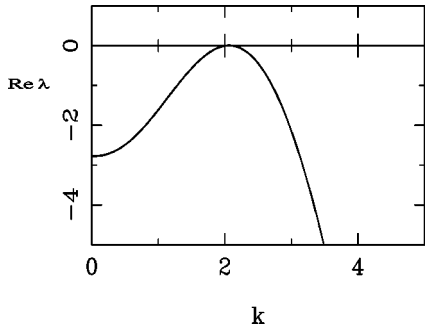

FIG. 6. Growth rate of Marangoni instability with short wavelength, $\mathrm{Re}\,\lambda$ versus k corresponding to model 1, for critical Marangoni number $M_{cr} = 750$ and $L = 1/120$. For sharp interfaces, the Marangoni instability develops around $k = 2$.

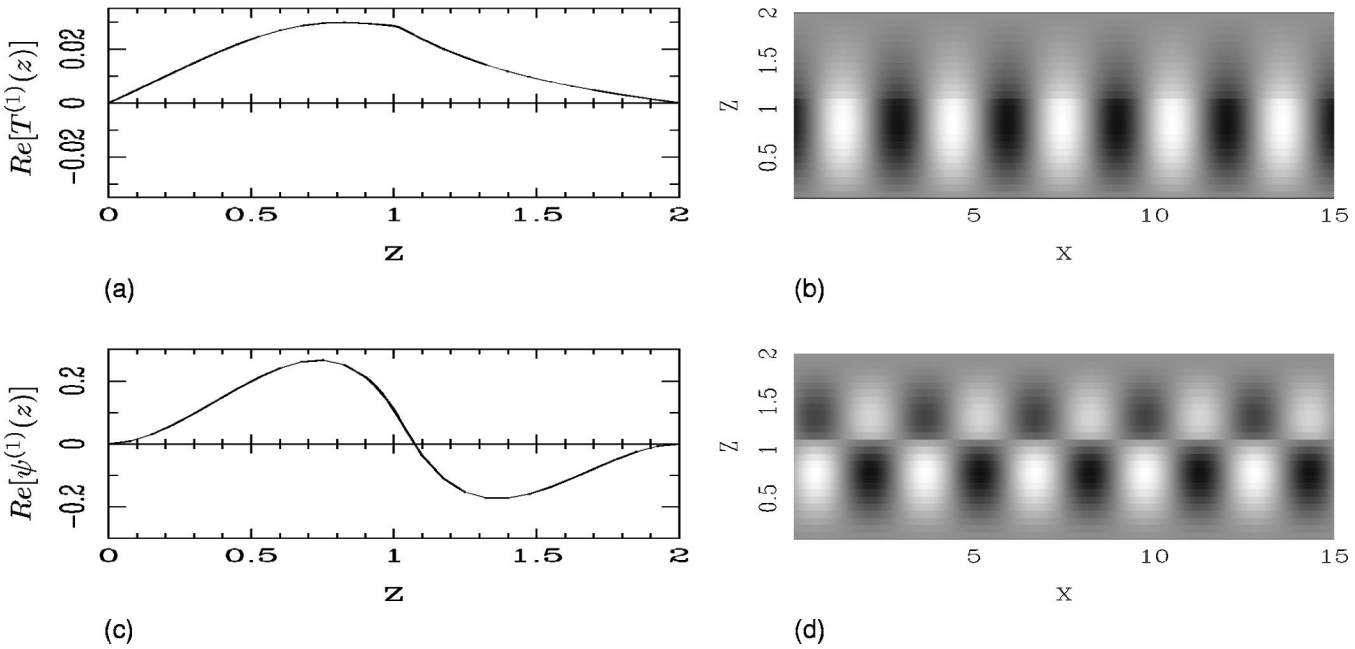

FIG. 7. Temperature perturbation [(a), (b)] and stream-function perturbation [(c), (d)] for short wave instability, corresponding to model 1, when the liquid-gas interface is perfectly rigid ($M=750$, $L=1/120$, $k=2.06$). Left panels plot the perturbations versus z and right panels present the same perturbations in the (x,z) representation. Thermocapillarities determine two convective motions: one in the liquid and one in the gas.

Fig. 7(a) expresses the heat-flux continuity condition [see relation (28) demonstrated in the sharp-interface limit in Sec. III], which is satisfied in our model without a supplementary restriction in this direction. Similarly, we observe in Fig. 7(c) a zero at the interface for the stream function ψ. Because $v_z=-\partial\psi/\partial x=-ik\psi$, $\psi=0$ along $z=1$ means $v_z=0$ at interface, a fact that emphasizes the fulfillment of the nondeformability condition (23). [Again, condition (23) is satisfied without imposing explicitly this interface condition in our formalism.]

In Figs. 7(b) and 7(d), the amplitude of the eigenfunctions belonging to the most dangerous modes are plotted in gray scale. Figure 7(d) is very suggestive because, as we have previously specified, the stream function ψ describes in fact the velocity component v_z. From this picture one observes two convective motions: one developed in the liquid and the other in the gas, a pattern specific for the short-wavelength instability.

For the sake of completeness, we have displayed in Figs. 8 and 9 the same representation as in Figs. 6 and 7, for the same instability, corresponding now to model 2. Figure 8 emphasizes again as how, in the sharp-interface limit, the classical results are reobtained: the short wave instability develops around $k=2$ for a critical Marangoni number $M_{cr}=750$. Figure 9 presents the perturbations for temperature, phase-field, and stream function, described by model 2. In this case, the liquid-gas interface is quasi-nondeformable. This means that the perturbations for the phase-field function exist but they are very small, of the order of 10^{-4} [see Fig. 9(c)], while the other perturbation profiles (for temperature and stream function) represented in Figs. 9(a), 9(b), 9(e), and 9(f) keep the same shapes such as those indicated by model 1 in Fig. 7.

B. Deformable interface

For small values of the capillary number Ca and the Galileo number G, the liquid-gas interface becomes deformable and surface deflections in the presence of a temperature gradient induce a second type of instability, developed around $k=0$, as one can see in Fig. 10. This is Marangoni convection with long wavelength, depicted in Fig. 10 for a liquid depth $d\approx 10^{-5}$ m. For this kind of instability, Fig. 11(c) reveals strong perturbations of the phase-field function (of the order of 10^{-1}), which means that the liquid-gas interface is deformed now. Even for small Marangoni numbers, these surface deflections lead to cellular convective motions developed in almost all liquid-gas systems, which is very suggestive as indicated by Fig. 11(f). This convective motion on a

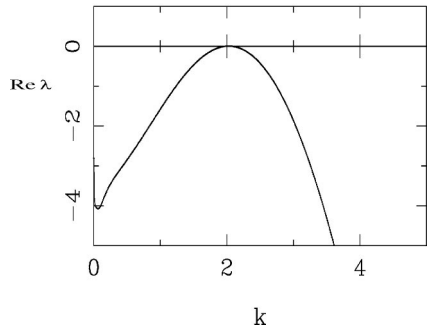

FIG. 8. Plot of growth rate for MC with short wavelength, Re λ versus k for quasi-nondeformable interface, in the limit of sharp interfaces ($L=1/60$) for the critical Marangoni number $M_{cr}=750$, $\mathrm{Ca}=2\times10^{5}$, and $G=3\times10^{9}$. Model 2 emphasizes the same result showed by model 1: the short wave instability arises around $k=2$.

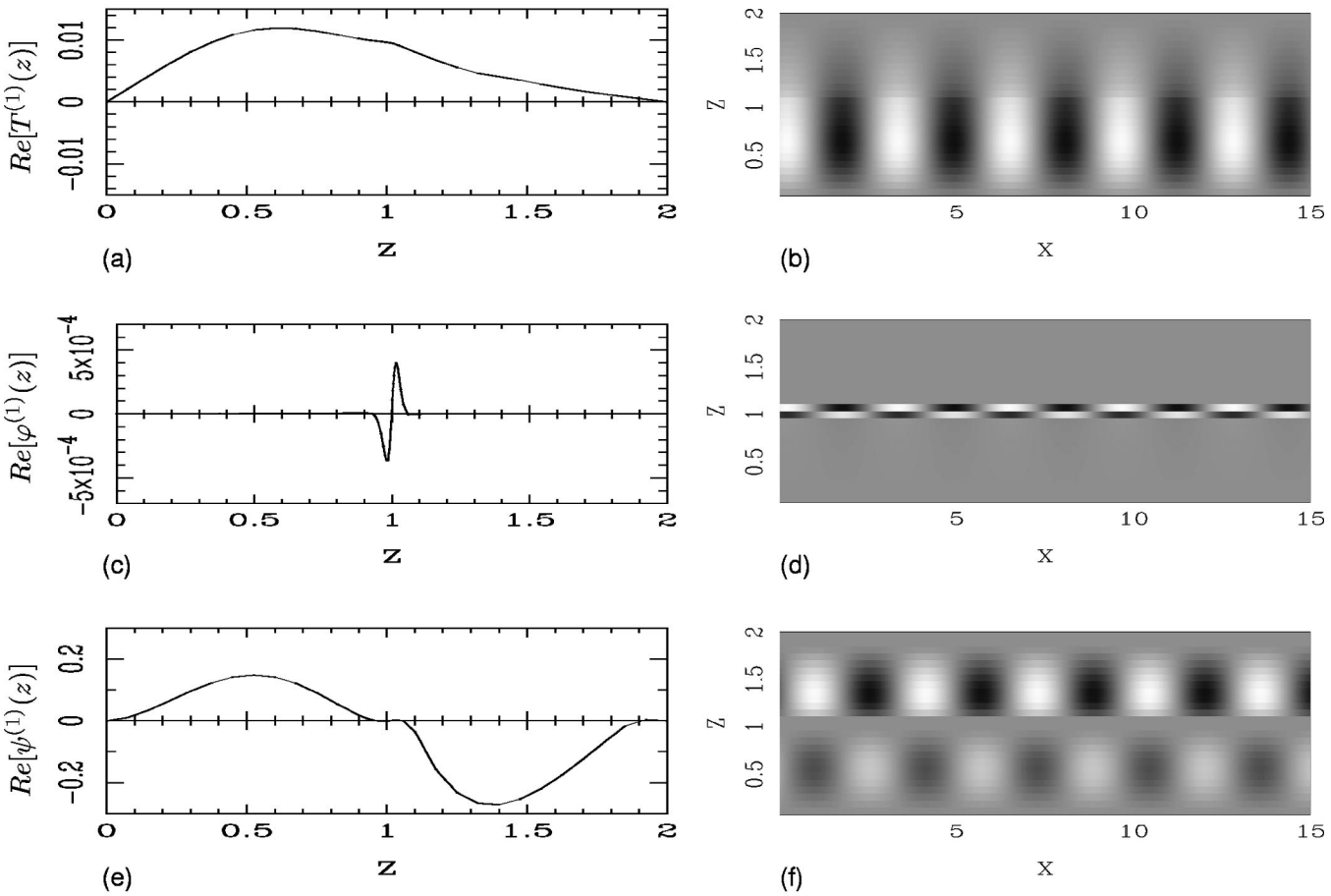

FIG. 9. Same as Fig. 7, but for model 2, when the liquid-gas interface is quasi-nondeformable ($M=750$, $L=1/60$, $k=2$, $\mathrm{Ca}=2\times10^5$, $G=3\times10^9$). Panels (a) and (b) illustrate the temperature perturbation, (c) and (d) the phase-field perturbation, and (e) and (f) the stream-function perturbation. In this case, the phase-field perturbations exist but they are very small, while the perturbation profile for temperature and stream function correspond with those presented in Fig. 7.

spatial scale much larger than the liquid layer depth is specific for long wave instability.

VI. CONCLUSIONS

Used in the previous works for studying alloy solidification, dendritic crystal growth, or dynamic fractures, the phase-field model is adjusted in this paper for describing Marangoni convection developed in two-fluid systems with a deformable interface heated from below. Adequate to multiphase systems, for which the interface location cannot be explicitly tracked, the phase-field method treats the problems in a continuous way, like an entire system, simplifying thus the system of equations and avoiding the interface conditions—the essential advantages of this method. Note that the shape of the interface can take arbitrary geometries and must not even be contiguous. Extensions of this method should allow, for example, for the description of drops or gas bubbles inside a liquid in an external temperature or concentration field. Therefore, the phase-field method has a much higher flexibility than the sharp-interface method, where the interface is described by a function of horizontal coordinates and is usually restricted to small deviations from the flat interfaces. In the frame of Lagrangian formalism, we have demonstrated in Sec. II the necessity to introduce in the Navier-Stokes equation a new force component $\frac{1}{2}\mathcal{K}_T\vec{\nabla}T(\vec{\nabla}\varphi)^2$ which is the driver of Marangoni convection with short wavelength. In the limit of sharp and rigid interfaces, we derived in Sec. III the classical interface conditions, starting from NS equation (18) with the above term included.

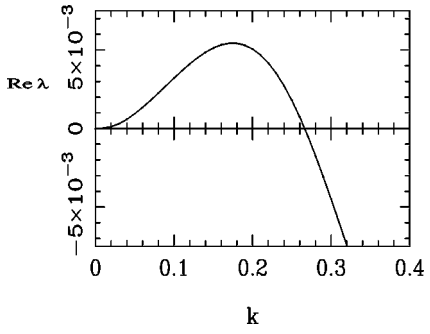

FIG. 10. Growth rate of the Marangoni instability with long wavelength $\mathrm{Re}\,\lambda$ versus wave number k when $M=8$, $L=2/9$, $\mathrm{Ca}=200$, $G=3$. For small values of capillary and Galileo numbers, a second convective instability develops around $k=0$.

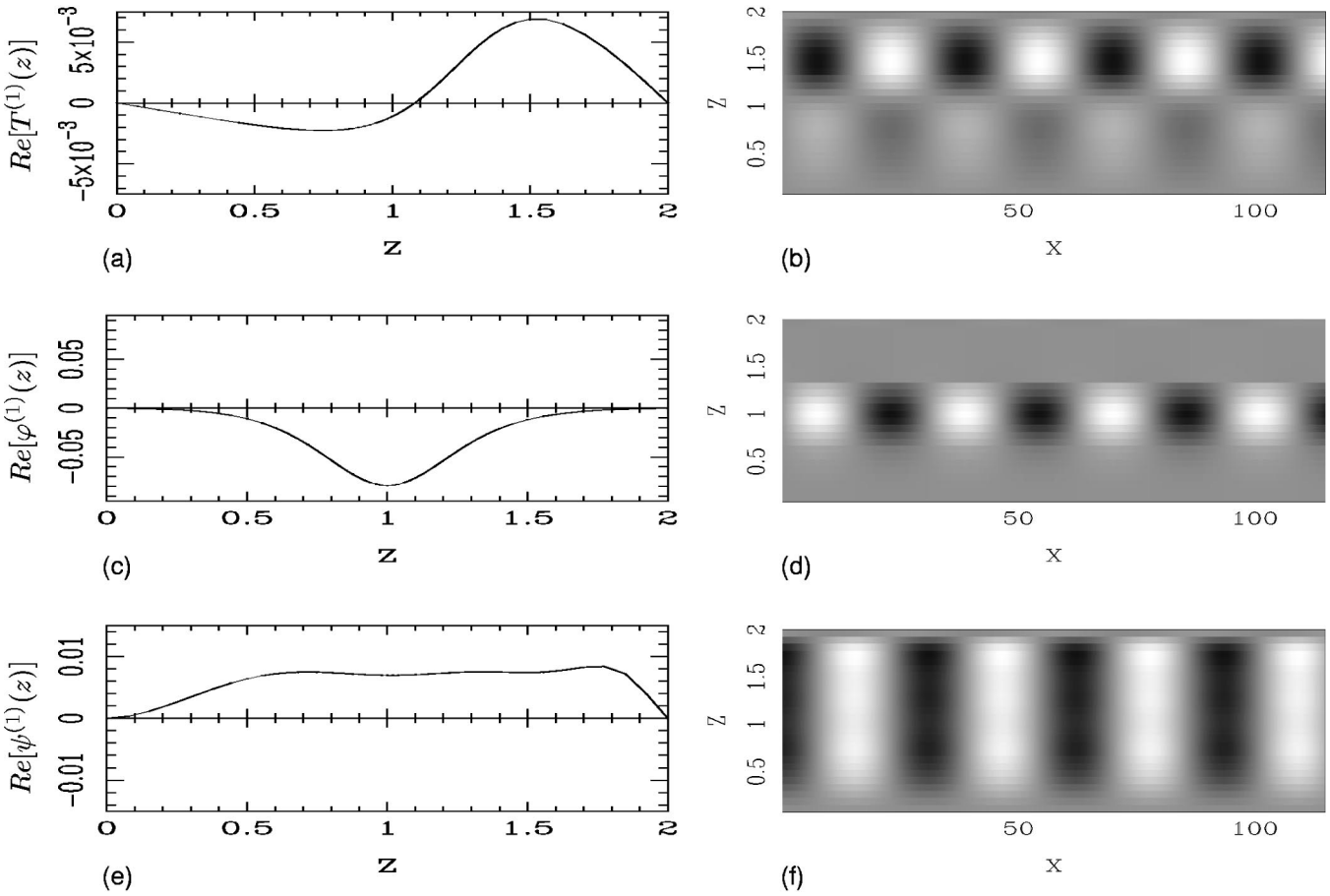

FIG. 11. Temperature [(a),(b)], phase-field [(c),(d)], and stream-function perturbations [(e),(f)] for long wave instability versus z (in left panels) and bidimensional (x,z) representations (in the right panels) when $M=8$, $k=0.2$, $L=2/9$, $\mathrm{Ca}=200$, $G=3$. The phase-field perturbations are strong now and, surface deformations in the presence of temperature gradient induce a convective motion in the whole liquid-gas system.

We have performed a numerical code for the bidimensional problem in the linear approximation, which models both Marangoni instabilities: one driven by surface tension gradients at the interface (short wave instability) and the second induced by surface deflections (long wave instability). Our numerical results emphasize on, in the sharp-interface limit, how the phase-field model applied for Marangoni convection leads to the results given by regular models for systems with flat interfaces [5]. This work will be continued in several directions: nonlinear effects will be included as well as the influence of evaporation through the interface, which can be considered in this approach in a more natural way.

ACKNOWLEDGMENT

This research was supported by the European Union under the network ICOPAC (Interfacial Convection and Phase Change) Grant No. HPRN-CT-2000-00136.

[1] H. Bénard, Rev. Gen. Sci. Pures Appl. **11**, 1261 (1900).
[2] M. Bestehorn, Phys. Rev. E **48**, 3622 (1993).
[3] S.J. VanHook *et al.*, Phys. Rev. Lett. **75**, 4397 (1995).
[4] S.K. Wilson and A. Thess, Phys. Fluids **9**, 2455 (1997).
[5] A.A. Golovin, A.A. Nepomnyashchy, and L.M. Pismen, J. Fluid Mech. **341**, 317 (1997).
[6] W.A. Tokaruk, T.C.A. Molteno, and S.W. Morris, Phys. Rev. Lett. **84**, 3590 (2000).
[7] M. Bestehorn and P. Colinet, Physica D **145**, 83 (2000).
[8] A. Engel and J.B. Swift, Phys. Rev. E **62**, 6540 (2000).
[9] V.C. Regnier, P.C. Dauby, and G. Lebon, Phys. Fluids **12**, 2787 (2000).
[10] J.S. Langer, in *Directions in Condensed Matter*, edited by G. Grinstein and G. Mazenko (World Scientific, Singapore, 1986), p. 165.
[11] R.J. Braun and B.T. Murray, J. Cryst. Growth **174**, 41 (1997).
[12] X. Tong, C. Beckermann, A. Karma, and Q. Li, Phys. Rev. E **63**, 061601 (2001).
[13] A. Karma, D.A. Kessler, and H. Levine, Phys. Rev. Lett. **87**, 045501 (2001).

[14] R. Fedkiw, T. Aslam, B. Merriman, and S. Osher, J. Comput. Phys. **152**, 457 (1999).
[15] R. Caiden, R. Fedkiw, and C. Anderson, J. Comput. Phys. **166**, 1 (2001).
[16] D. Jou, J. Casas-Vásquez, and G. Lebon, *Extended Irreversible Thermodynamics* (Springer-Verlag, Berlin, 1993).
[17] D.M. Anderson, G.B. McFadden, and A.A. Wheeler, Annu. Rev. Fluid Mech. **30**, 139 (1998).
[18] D. Jasnow and J. Viñals, Phys. Fluids **8**, 660 (1996).
[19] J.S. Rowlinson and B. Widom, *Molecular Theory of Capillarity* (Clarendon Press, Oxford, 1982), p. 56.
[20] J. Lowengrub and T. Truskinovsky, Proc. R. Soc. London, Ser. A **454**, 2617 (1998).
[21] A.A. Wheeler and G.B. McFadden, Proc. R. Soc. London, Ser. A **453**, 1611 (1997).
[22] D.M. Anderson, G.B. McFadden, and A.A. Wheeler, Physica D **135**, 175 (2000).
[23] P. Colinet, J.C. Legros, and M.G. Velarde, *Nonlinear Dynamics of Surface-Tension Driven Instabilities* (Wiley-VCH, Berlin, 2001), p. 31.
[24] C. Hirsch, *Numerical Computation of Internal and External Flows* (Wiley, New York, 1998), Vol. 1, p. 201.